Biochemical and Biophysical Research Communications 379 (2009) 76–80

Contents lists available at ScienceDirect

Biochemical and Biophysical Research Communications

journal homepage: www.elsevier.com/locate/ybbrc

Structural basis for the broad range substrate specificity of a novel mouse cytosolic sulfotransferase—mSULT1D1

Takamasa Teramoto [a], Yoichi Sakakibara [b], Ming-Cheh Liu [c], Masahito Suiko [b], Makoto Kimura [a,d], Yoshimitsu Kakuta [a,d,*]

[a] Laboratory of Structural Biology, Department of Systems Life Sciences, Graduate School, Faculty of Agriculture, Kyushu University, Hakozaki 6-10-1, Higashi-ku, Fukuoka 812-8581, Japan
[b] Food Research Branch, Department of Biochemistry and Applied Biosciences, Faculty of Agriculture, University of Miyazaki, Miyazaki 889-2192, Japan
[c] Department of Pharmacology, College of Pharmacy, The University of Toledo, Toledo, OH 43606, USA
[d] Laboratory of Biochemistry, Department of Bioscience and Biotechnology, Graduate School, Faculty of Agriculture, Kyushu University, Hakozaki 6-10-1, Higashi-ku, Fukuoka 812-8581, Japan

ARTICLE INFO

Article history:
Received 19 November 2008
Available online 13 December 2008

Keywords:
Broad range substrate specificity
Cytosolic sulfotransferase
SULT
Crystal structure
Sulfonation

ABSTRACT

The mouse cytosolic sulfotransferase, mSULT1D1, catalyzes the sulfonation of a wide range of phenolic molecules including *p*-nitrophenol (*p*NP), α-naphthol (αNT), serotonin, as well as dopamine and its metabolites. To gain insight into the structural basis for its broad range substrate specificity, we solved two distinct ternary crystal structures of mSULT1D1, complexed with 3′-phosphoadenosine-5′-phosphate (PAP) plus *p*NP or PAP plus αNT. The structures revealed that the mSULT1D1 contains an L-shaped accepter-binding site which comprises 20 amino acid residues and four conserved water molecules. The shape of the accepter-binding site can be adjusted by conformational changes of two residues, Ile148 and Glu247, upon binding with respective substrates.

In mammals, the cytosolic sulfotransferases (SULTs) play important roles in the Phase II detoxification of xenobiotics as well as in the homeostasis of catecholamine neurotransmitters and steroid/thyroid hormones [1,2]. SULTs utilize 3′-phosphoadenosine 5′-phosphosulphate (PAPS) as the sulfonate donor to catalyze the sulfonation of substrate compounds, yielding 3′-phosphoadenosine 5′-phosphate (PAP) and sulfonate conjugates. Based on their amino acid sequences, six distinct SULT gene families (designated SULT1 through 6) have been categorized and SULT1 represents the largest of the six SULT families [3]. Members of the SULT1 family enzymes have been shown to be capable of sulfonating a variety of small planar phenols including 17β-estradiol, thyroid hormones, serotonin, catecholamines as well as certain environmental xenobiotics and drugs such as minoxidil. Studies have shown that not all SULT1 members are present in all mammalian species. In particular, SULT1D1 is found in mice [4] and dogs [5], but not in humans [6].

In mice, mSULT1D1 has a widespread tissue distribution [7] and has been shown to metabolize catecholamines [8,9] and play a significant role in the metabolism of a broad range of xenobiotics such as *p*-nitrophenol (*p*NP), α-naphthol (αNT) [4,10]. We have recently reported the first crystal structure of mSULT1D1 in complex with PAP, and clarified how mSULT1D1 can recognize dopamine as a substrate [11]. In that study, a water molecule which interacts with the main chain of Ile148 and Glu247 was found to be strongly involved in recognition of dopamine by mSULT1D1 [11]. How mSULT1D1 can accommodate other endogenous or xenobiotic substrate that are structurally distinct from dopamine, however, remains unclear.

To better understand the structural basis for its broad range substrate specificity, we attempted to determine the crystal structure of mSULT1D1 in complex with a variety of xenobiotics. We succeeded in the determination of the crystal structures of mSULT1D1 complexed with PAP plus *p*NP or αNT. Data obtained revealed that the enzyme contains two sites that recognize small phenolic ring in its substrate binding pocket and two key amino acid residues, Ile148 and Glu247, may undergo conformational changes upon binding with different substrate. The mechanism underlying the broad range substrate specificity of mSULT1D1 is proposed based on the two newly determined crystal structures.

Materials and methods

Cloning, expression, purification, and crystallization of recombinant mSULT1D1. Procedures for the cloning, expression, purification, and crystallization of recombinant mSULT1D1 have previously been

* Corresponding author. Fax: +81 92 642 2854.
E-mail address: kakuta@agr.kyushu-u.ac.jp (Y. Kakuta).

0006-291X/$ - see front matter © 2008 Elsevier Inc. All rights reserved.
doi:10.1016/j.bbrc.2008.12.013

reported [11]. In brief, crystallization of the enzyme was carried out as follows. Single crystals were grown by the hanging-drop vapor diffusion method. The protein solution was composed of 8 mg/ml of purified mSULT1D1 in 50 mM Tris–HCl, pH 7.9, 150 mM NaCl, 10 mM dithiothreitol, and 5 mM PAP. After mixing protein and reservoir solutions (16% PEG 10000, 10 mM DTT and 100 mM Bis-Tris, pH 5.5) in a 1:1 ratio, crystals were grown following three days of incubation at 20 °C.

Preparation of mSULT1D1 crystal complexed with PAP plus pNP or αNT. mSULT1D1 crystals co-crystallized with PAP were soaked into saturated *p*NP or αNT solution (50 mM Tris–HCl, pH 7.9, 150 mM NaCl, 10 mM dithiothreitol, 5 mM PAP, 16% PEG 10000, 100 mM Bis-Tris, pH 5.5, 25% glycerol, and saturated with *p*NP or αNT) for 1 h prior being used for structural determination.

Data collection. Each of the two mSULT1D1 crystals, prepared as described above, was mounted on a cryo-loop, then flash-cooled with a nitrogen gas stream at 100 K. X-ray diffraction data was collected with a ADSC CCD and synchrotron radiation at BL38B1, SPring-8. The diffraction data were processed using the program package HKL2000 [12]. Both crystals were found to belong to the space group *C*2. Data collection statistics are summarized in Table 1.

Structure determination and refinement. The crystal structures of mSULT1D1-PAP-*p*NP and mSULT1D1-PAP-αNT were determined by molecular replacement using a previously reported mSULT1D1-PAP structure (Protein Data Bank code: 2ZPT) as a search model with the program Molrep [13]. The structures were refined using Refmac5 [14] with diffraction data from 23.4 to 1.3 Å for mSULT1D1-PAP-*p*NP and 21.4–1.3 Å for mSULT1D1-PAP-αNT. Iterative cycles of refinements and manual rebuilding in Coot [15] were carried out until the free R-factor converged. Stereochemical checks were carried out using PROCHECK [16]. Refinement statistics are summarized in Table 1. The atomic coordinates and structure factors of mSULT1D1-PAP-*p*NP and mSULT1D1-PAP-αNT have been deposited in the Protein Data Bank at Rutgers University under accession code 2ZVP and 2ZVQ, respectively.

Table 1
Data collection and refinement statistics.

Data collection	PAP–*p*NP	PAP–αNT
Space group	*C*2	*C*2
Unit cell parameters	a = 156.5 Å, b = 67.6 Å, c = 42.7 Å, β = 105.5°	a = 156.2 Å, b = 67.5 Å, c = 42.8 Å, β = 105.5°
Beam line	SPring-8 BL38B1	SPring-8 BL38B1
Wavelength (Å)	1.000	1.000
Resolution range (Å)	50.0–1.3	50.0–1.23
Number of reflections		
Observed/Unique	270,484/87,253	307,686/96,125
Redundancy	3.1 (1.8)	3.2 (1.2)
R_{sym}[a,b]	0.079 (0.507)	0.061 (0.743)
$I/\sigma(I)$[a]	20.4 (0.8)	13.4 (0.5)
Completeness (%)	83.0 (34.8)	77.6 (9.0)
Refinement statistics		
Resolution range (Å)	23.4–1.3	21.4–1.3
Number of reflections		
Working set/Test set	82,904/4339	89,192/4677
Completeness (%)	83.0	89.3
R_{cryst}[c] (%)/R_{free}[d] (%)	17.5/19.0	17.3/18.9
Root mean square deviations		
Bond length (Å)/Bond angles (°)	0.008/1.2	0.008/1.2
Average B-factor (Å^2)/Number of atoms		
Protein	13.9/2616	11.3/2592
PAP	9.4/27	7.5/27
Acceptor substrate		
*p*NP^1	14.3/10	
*p*NP^2	21.4/10	
αNT^1		11.4/11
αNT^2		8.7/11
αNT^3		13.7/11
αNT^4		6.9/11
Glycerol	49.1/6	26.9/12
Water	27.7/355	27.2/424
Ramachandran analysis		
Most favored (%)	92.0	92.2
Allowed (%)	8.0	7.8
Generously allowed (%)	0.0	0.0
Disallowed (%)	0.0	0.0

[a] Values in parentheses are for the highest-resolution shell.
[b] $R_{sym} = \sum(I - \langle I\rangle)/\sum\langle I\rangle$, where I is the intensity measurement for a given refraction and $\langle I\rangle$ is the average intensity for multiple measurements of this refraction.
[c] $R_{cryst} = \sum|F_{obs} - F_{cal}|\ \sum F_{obs}$, where F_{obs} and F_{cal} are observed and calculated structure factor amplitudes.
[d] R_{free} value was calculated for R_{cryst}, using only an unrefined randomly chosen subset of reflection data (5%).

Results

Overall structure

Crystals complexed with PAP plus *p*NP or PAP plus αNT diffracted up to 1.3 Å and the final structures were refined to R_{work}/R_{free} values of 17.3%/19.0% and 17.3%/18.9%, respectively (Table 1). Superposition of the mSULT1D1-PAP structure [11] with those from mSULT1D1-PAP-*p*NP or mSULT1D1-PAP-αNT revealed the root-mean-square deviations (rmsd) value of 0.21 Å for 287 Cα and 0.20 Å for 285 Cα, respectively. The overall structures of mSULT1D1-PAP-*p*NP and mSULT1D1-PAP-αNT were identical to that of mSULT1D1-PAP and residues surrounding the PAPS binding site remains structurally unchanged (Fig. 1A) [17].

*p*NP binding

The mSULT1D1-PAP-*p*NT crystal structure revealed the presence of two *p*NP molecules (designated *p*NP^1 and *p*NP^2) in accepter substrate binding site (Fig. 1C), similar to the previously reported crystal structure of human SULT1A1 (hSULT1A1) complexed with two *p*NP molecules [18].

Compared with mSULT1D1-PAP complex (Figs. 1B and 2A) [11], different conformations of Ile148 and Glu247 in the mSUTL1D1-PAP-*p*NP complex, designated Ile148^{type2} and Glu247^{type2}, (Figs. 1C and 2B), were clearly observed. It was noted that the conformations of these residues in SULT1D1-PAP complex, designated Ile148^{type1} and Glu247^{type1}, (cf. Figs. 1B and 2A), would have induced steric clashes with the nitro groups of *p*NP^1 and *p*NP^2, respectively.

In mSULT1D1-PAP-*p*NP complex, *p*NP^1 was bound in a catalytically competent manner, with identical position and orientation to those of the *p*NP^1 in hSULT1A1 [18]. Two residues, Phe142 and Phe81 sandwiched the aromatic ring of *p*NP^1 (Fig. 1C). These two hydrophobic residues shaped a substrate access gate that may allow only planar substrates to bind in a productive or catalytic orientation. The phenolic hydroxyl of *p*NP^1 formed hydrogen bonds with the side chains of catalytic residues His108 and Lys106 and with a well-ordered water molecule (Wat1) which also interacted with an oxygen of the 5′-phosphate group of PAP. The nitro group of *p*NP^1 interacted with a water molecule (Wat2) and formed van der Waals interactions with Phe21, Ile148, and His149.

In contrast, *p*NP^2 did not form hydrogen bonds with any of the catalytic residues. Instead, the phenolic hydroxyl of *p*NP^2 formed hydrogen bonds with two conserved ordered water molecules (Wat3 and Wat4). The phenolic ring formed hydrophobic interactions with the side chains of Leu84 and Met243, and the nitro group formed van der Waals interactions with Ile86, Ile89, and

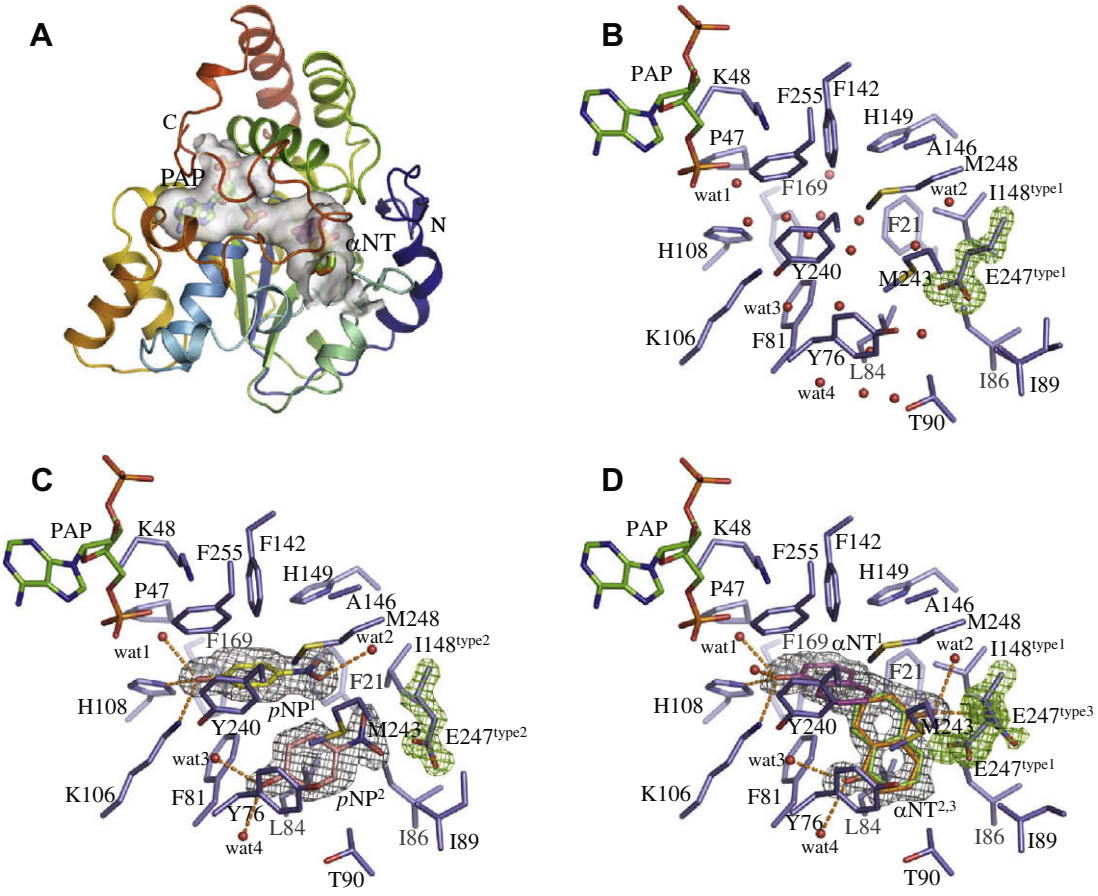

Fig. 1. Overall structure of SULT1D1-PAP-α-naphthol (αNT) (A). Inner surface for donor substrate product PAP and accepter substrate αNT are shown in gray wall. Acceptor substrate-binding site of (B) SULT1D1–PAP complex, (C) SUTL1D1–PAP–*p*NP complex, and (D) SULT1D1–PNP–αNT complex. Residues are shown in stick model. All atoms of residues are shown in red and blue for oxygen and nitrogen, respectively. *p*NP molecules is shown in stick model with two colors: pNP^1 (yellow) and pNP^2 (pink). αNT are shown in stick model with three colors: αNT^1 (purple), αNT^2 (green), and αNT^3 (orange). The conserved water molecules are shown in ball model in red. (For interpretation of the references to color in this figure legend, the reader is referred to the web version of this article.)

Glu247 (Fig. 1C). The orientation of pNP^2 in mSULT1D1-PAP-*p*NP was different from that of pNP^2 bound with hSULT1A1 [18]. Compared with pNP^2 in hSULT1A1, pNP^2 in mSULT1D1 rotated 90° to bind in the substrate binding site.

αNT binding

A clear Fo-Fc electron density of αNT was observed for the mSULT1D1-PAP-αNT complex after the first refinement cycle. The observation revealed the presence of three αNT molecules (αNT^1, αNT^2, and αNT^3) in the substrate-binding site (Fig. 1D) and one αNT molecule (αNT^4) near C-terminal region. The αNT^4 was located on surface of mSULT1D1 and away from the substrate-binding site. The three αNT molecules (αNT^1, αNT^2, and αNT^3) seemed not to be able to bind simultaneously in the substrate-binding pocket, because their binding areas overlapped one another (Fig. 1D). Therefore, during refinement process, we have determined the occupancy and B-factor of these αNT molecules (αNT^1: occupancy 0.6, B-factor 11.4 Å^2, αNT^2: occupancy 0.2, B-factor 8.7 Å^2, and αNT^3: occupancy 0.2, B-factor 13.7 Å^2).

Glu247 could assume two conformations (occupancy 0.6 for $Glyu247^{type1}$: Fig. 2C and 0.4 for $Glu247^{type3}$: Fig. 2D) in response to different ways of binding with αNT. In the case of binding with αNT^1, $Glu247^{type1}$ was taken, whereas in the case of binding with αNT^2 or αNT^3, $Glu247^{type3}$ was taken. This might have been because αNT^2 and αNT^3 would cause steric hindrance with $Glu247^{type1}$ and $Glu247^{type2}$.

αNT^1 was bound in a catalytically competent manner, and its phenolic ring was oriented within the active site in the same way as that found with pNP^1. The phenolic hydroxyl group of αNT^1 formed hydrogen bonds with the side chains of catalytic residues His108 and Lys106 and a conserved water molecule (Wat1) (Fig. 1D), and the aromatic ring formed van der Waals interactions with Met248.

In contrast, αNT^2 and αNT^3 formed no interactions with the catalytic residues. While the naphthalene framework of αNT^2 and αNT^3 bound in identical positions, the locations of their hydroxyl groups were different. The phenolic hydroxyl group of αNT^2 formed hydrogen bonds with two ordered water molecules (Wat3 and Wat4). The phenolic hydroxyl group of αNT^3 formed hydrogen bonds with one of the conformation of Glu247 ($Glu247^{type3}$) as well as an ordered water molecule (Wat2). Interestingly, one of the aromatic rings of naphthalene framework of αNT^2 and αNT^3 was in a position identical that of to pNP^2 in mSULT1D1-PAP-*p*NP complex.

Discussion

From the two ternary crystal structures determined in this study, it can be concluded that the substrate-binding pocket surface of mSULT1D1 is formed by 17 hydrophobic residues (Phe21, Pro47, Tyr76, Phe81, Leu84, Ile86, Ile89, Thr90, Phe142, Ala146, Ile148, His149, Phe169, Tyr240, Met243, Met248, and Phe255), two catalytic residues (Lys106 and His108), one hydrophilic reside

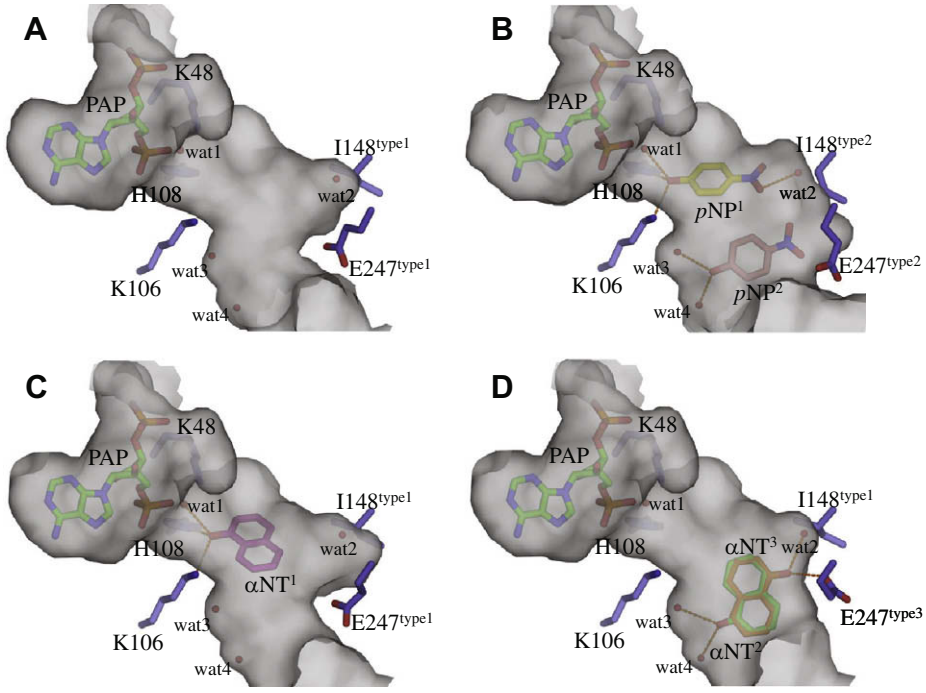

Fig. 2. Inner surface representation of multiple structures of mSULT1D1 depending on Glu247 and Ile148 conformational change. (A) Previous determined PAP complex. (B) PAP–*p*NP^1 and *p*NP^2 complex structure. (C) PAP–αNT^1 complex, and (D) PAP–αNT^2 or αNT^3 complex. Residues are shown in stick model. All atoms of residues are shown in red and blue for oxygen and nitrogen, respectively. *p*NP molecules is shown in stick model with two colors: *p*NP^1 (yellow) and *p*NP^2 (pink). αNT are shown in stick model with three colors: αNT^1 (purple), αNT^2 (green), and αNT^3 (orange). The conserved water molecules are shown in ball model in red. (For interpretation of the references to color in this figure legend, the reader is referred to the web version of this article.)

(Glu247), and four structurally conserved water molecules (Wat1, Wat2, Wat3, and Wat4). It appears that the shape of the hydrophobic wall and the position of hydrophilic areas in the substrate-binding pocket define the substrate specificity of mSULT1D1. Hydrophilic parts of the substrates, including hydroxyl, carbonyl, carboxyl, amino, and imino groups, can form interactions with hydrophilic residues and/or conserved water molecules. In our previous study, we had indeed demonstrated that a water molecule (Wat2) plays a critical role in the recognition of the amine group of dopamine [11].

The two kinds of conformational changes of Ile148 (type 1 and 2) and the three kinds of conformational changes of Glu247 (type 1, 2, and 3) may vary both the shape and hydrophilic area locations of the accepter substrate-binding site of mSULT1D1 (Fig. 2A–D). Such conformational variations of the substrate-binding pocket may expand the diversity of substrates capable of binding to the substrate-binding pocket. While Glu247 interacted with *p*NP^2 and αNT^3 whose bindings result in no catalytic consequences, the conformational change of Glu247 may contribute to the determination of the substrate-binding affinity and the position for longer substrate such as catecholamines, serotonin or minoxidil. In fact, we had previously reported a dopamine-binding model and shown that Glu247 could interact with the amine group of dopamine. Therefore, the conformational changes of Glu247 may expand the range of substrate and contribute to the broad substrate specificity of mSULT1D1.

The conformational changes of a specific residue present in the accepter-binding pocket have also been reported in hSULT1A1 structures [18,19]. In hSULT1A1, Phe247 adopted an alternate rotamer conformation upon binding with *p*NP or 17β-estradiol. Phe247 of hSULT1A1 is conformationally equivalent to Glu247 of mSULT1D1. Our results suggest that the position for conformational change is conserved in both hSULT1A and mSULT1D subfamilies. The movement should have some important role for the broad range substrate specificity. In view of that the broad range substrate specificity is a common feature for members of different SULT families, the information derived from our current study may help understand the broad substrate specificities of other SULT enzymes.

Acknowledgments

We thank Drs. K. Hasegawa and H. Sakai of the Japan Synchrotron Radiation Research Institute (JASRI) for the kind assistance with data collection using the synchrotron radiation of BL38B1, SPring-8. Synchrotron radiation experiments were carried out with JASRI approval.

This research was supported by the Grant-in-Aid for Scientific Research and the National Project on Protein Structural and Functional Analyses from the Ministry of Education, Culture, Sports, Science and Technology, Japan.

References

[1] M.W. Coughtrie, S. Sharp, K. Maxwell, N.P. Innes, Biology, function of the reversible sulfation pathway catalysed by human sulfotransferases, sulfatases, Chem. Biol. Interact. 109 (1998) 3–27.
[2] C.N. Falany, Enzymology of human cytosolic sulfotransferases, FASEB J. 11 (1997) 206–216.
[3] R.L. Blanchard, R.R. Freimuth, J. Buck, R.M. Weinshilboum, M.W. Coughtrie, A proposed nomenclature system for the cytosolic sulfotransferase (SULT) superfamily, Pharmacogenetics 14 (2004) 199–211.
[4] Y. Sakakibara, K. Yanagisawa, Y. Takami, T. Nakayama, M. Suiko, M.C. Liu, Molecular cloning, expression, and functional characterization of novel mouse sulfotransferases, Biochem. Biophys. Res. Commun. 247 (1998) 681–686.
[5] C. Tsoi, C.N. Falany, R. Morgenstern, S. Swedmark, Identification of a new subfamily of sulphotransferases: Cloning and characterization of canine SULT1D1, Biochem. J. 356 (2001) 891–897.
[6] W. Meinl, H. Glatt, Structure, localization of the human SULT1B1 gene: neighborhood to SULT1E1 and a SULT1D pseudogene, Biochem. Biophys. Res. Commun. 288 (2001) 855–862.
[7] Y. Alnouti, C.D. Klaassen, Tissue distribution, ontogeny of sulfotransferase enzymes in mice, Toxicol. Sci. 93 (2006) 242–255.
[8] M. Shimada, R. Terazawa, Y. Kamiyama, W. Honma, K. Nagata, Y. Yamazoe, Unique properties of a renal sulfotransferase, St1d1, in dopamine metabolism, J. Pharmacol. Exp. Ther. 310 (2004) 808–814.

[9] H.M. van den Bosch, M. Bunger, P.J. de Groot, J. van der Meijde, G.J. Hooiveld, M. Muller, Gene expression of transporters and phase I/II metabolic enzymes in murine small intestine during fasting, BMC Genomics 8 (2007) 267.
[10] M.C. Liu, Y. Sakakibara, C.C. Liu, Bacterial expression, purification, and characterization of a novel mouse sulfotransferase that catalyzes the sulfation of eicosanoids, Biochem. Biophys. Res. Commun. 254 (1999) 65–69.
[11] T. Teramoto, Y. Sakakibara, K. Inada, K. Kurogi, M.C. Liu, M. Suiko, M. Kimura, Y. Kakuta, Crystal structure of mSULT1D1, a mouse catecholamine sulfotransferase, FEBS Lett. 582 (2008) 3909–3914.
[12] Z. Otwinowski, W. Minor, Processing of X-ray diffraction data collected in oscillation mode, Methods Enzymol. 276 (1997) 307–326.
[13] A. Vagin, A. Teplyakov, An approach to multi-copy search in molecular replacement, Acta Crystallogr. D Biol. Crystallogr. 56 (2000) 1622–1624.
[14] G.N. Murshudov, A.A. Vagin, E.J. Dodson, Refinement of macromolecular structures by the maximum-likelihood method, Acta Crystallogr. D Biol. Crystallogr. 53 (1997) 240–255.
[15] P. Emsley, K. Cowtan, Coot: model-building tools for molecular graphics, Acta Crystallogr. D Biol. Crystallogr. 60 (2004) 2126–2132.
[16] A.A. Vaguine, J. Richelle, S.J. Wodak, SFCHECK: a unified set of procedures for evaluating the quality of macromolecular structure-factor data and their agreement with the atomic model, Acta Crystallogr. D Biol. Crystallogr. 55 (1999) 191–205.
[17] Y. Kakuta, L.G. Pedersen, C.W. Carter, M. Negishi, L.C. Pedersen, Crystal structure of estrogen sulphotransferase, Nat. Struct. Biol. 4 (1997) 904–908.
[18] N.U. Gamage, R.G. Duggleby, A.C. Barnett, M. Tresillian, C.F. Latham, N.E. Liyou, M.E. McManus, J.L. Martin, Structure of a human carcinogen-converting enzyme, SULT1A1. structural and kinetic implications of substrate inhibition, J. Biol. Chem. 278 (2003) 7655–7662.
[19] N.U. Gamage, S. Tsvetanov, R.G. Duggleby, M.E. McManus, J.L. Martin, The structure of human, SULT1A1 crystallized with estradiol: an insight into active site plasticity and substrate inhibition with multi-ring substrates, J. Biol. Chem. 280 (2005) 41482–41486.